Chapter 13

In Vivo Quantification of Intramolecular FRET Using RacFRET Biosensors

Manel Bosch and Elena Kardash

Abstract

Genetically encoded FRET biosensors are powerful tools to visualize protein activity and signaling events in vivo. Compared with a biochemical approach, FRET biosensors allow a noninvasive spatial-temporal detection of signaling processes in live cells and animal tissues. While the concept of this technique is relatively simple, the experimental procedure is complicated and consists of several steps: (1) biosensor optimization; (2) data acquisition; and (3) image processing with each step posing its own challenge. In this chapter, we discuss steps (2) and (3) with the emphasis on the intramolecular RacFRET biosensor. We describe the design principle of the biosensor, the experimental imaging setup for acquiring FRET data in zebrafish embryos expressing the RacFRET biosensor, and the step-by-step ratio image generation protocol using *Fiji* software. We discuss important considerations during FRET data acquisition and analysis. Finally, we provide a macro code for the automated ratio image generation.

Key words FRET biosensors, Sensitized emission, FRET ratio imaging, Zebrafish, Rac, Rho GTPases, Fiji/ImageJ, Macro programming

1 Introduction

Förster resonance energy transfer (FRET) is an electrodynamic phenomenon of a non-radiative energy transfer that occurs between two fluorophores called donor and acceptor. FRET requires a spectral overlap between donor emission and acceptor absorption and occurs at a distance between donor and acceptor ranging from 10 to 100 Å. Additional conditions may apply such as certain relative orientations between the emission dipole of the donor and the absorption dipole of the acceptor but these are usually negligible when biological samples are concerned [1]. During FRET, the donor in the excited state transfers the energy to the acceptor in the ground state. As a result, the emission from the

Electronic supplementary material: The online version of this chapter (https://doi.org/10.1007/978-1-4939-9686-5_13) contains supplementary material, which is available to authorized users.

Elena Rebollo and Manel Bosch (eds.), *Computer Optimized Microscopy: Methods and Protocols*, Methods in Molecular Biology, vol. 2040, https://doi.org/10.1007/978-1-4939-9686-5_13,

donor molecule is reduced in the process called quenching while the emission from the acceptor is increased. These changes can be detected in a fluorescence microscope. The relative emission levels from donor and acceptor molecules upon donor excitation reflect FRET efficiency, which in turn can be used to measure the distances between molecules [1, 2].

One of the most common biological applications of FRET is to measure distances between molecules [3, 4]. FRET sensitivity allows to detect minute changes in macromolecules directly in living tissues otherwise not accessible by conventional imaging techniques such as those involving regular fusion proteins. This can be very useful when studying protein-protein interactions and protein conformational changes in living cells. Intramolecular FRET-based biosensors were specifically designed for investigating signaling pathways in real time. Since the creation of calmodulin—the first FRET biosensor for measuring calcium signaling in living cells [5]—multiple biosensors were designed aimed at deciphering a range of signaling pathways and protein activities in tissues and cells. Today we have access to numerous biosensor modules, among which are those to study kinases, Rho GTPases, neuronal activity, PH levels, and calcium signaling—just to name a few [4, 6–9]. In this chapter, we focus on the intramolecular FRET biosensors for measuring the activity of Rho GTPases [8, 10]; specifically we consider the RacFRET biosensor [11, 12].

Rac protein belongs to a family of Rho GTPases, which is a family of small proteins (about 21 kDa) that control multiple cellular processes ranging from cell migration and differentiation to endocytosis and cell division [10]. Rho GTPases exist in two main states: the active, GTP bound, and the inactive, GDP bound. In the active state, Rho GTPases form complexes with their effector proteins to induce signaling events controlling cellular physiology and behavior. Rac protein is one of the prominent Rho GTPases controlling actin polymerization during cell shape changes such as those involving cell migration [10]. There are several isoforms of Rac proteins, which may only differ in a few amino acids yet perform diverse functions. A number of FRET-based sensors were developed to study the activity of Rho GTPases in living cells [8, 11, 13, 14]. In the past decade, several modifications were introduced to Rac and RhoA biosensors to improve their sensitivity, accuracy, and dynamic range [12, 15–17]. It is important to remember that intramolecular FRET biosensors for Rho GTPases reflect the balance between GEF and GAP activities that would activate the respective endogenous Rho GTPase. These biosensors, while being unique to the specific Rho GTPase, might not differentiate between the closely related isoforms of the specific protein.

A typical FRET biosensor for Rho GTPase is a single-chain macromolecule consisting of two fluorescent proteins serving as donor and acceptor during the energy transfer linked together with

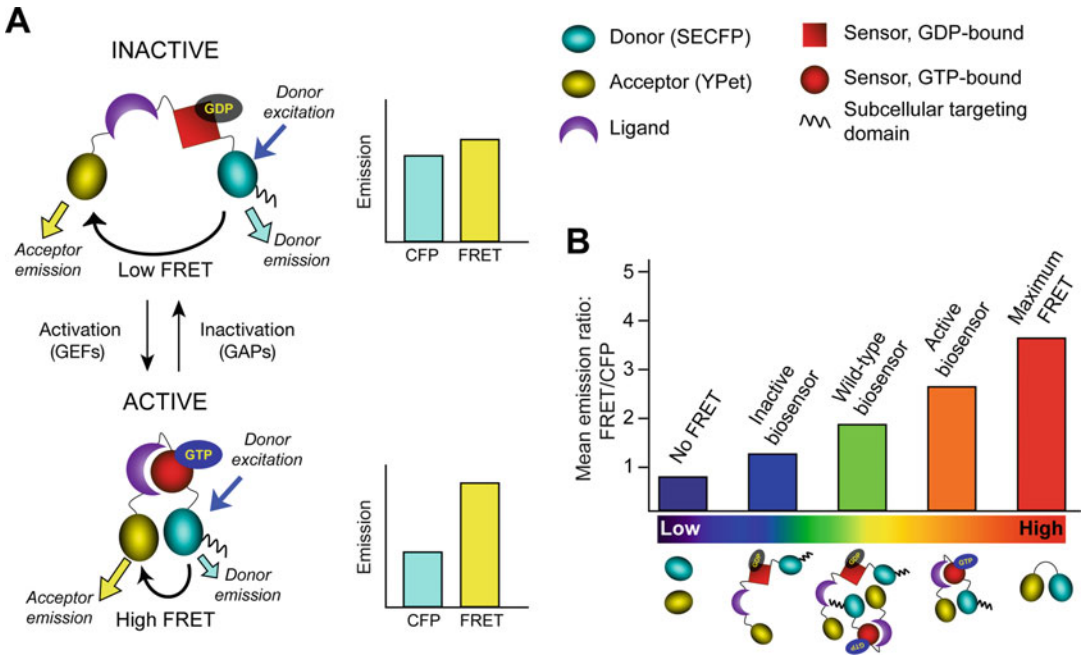

Fig. 1 The principal design of an intramolecular FRET biosensor for Rho GTPases. (**a**) The scheme shows a molecular chain consisting of two fluorophores, the YPet and the CFP fused to the sensor and ligand domains by flexible linkers. Sensor domain binds GDP or GTP moiety, which is controlled by the GAP and GEF groups of proteins, respectively. In the GTP-bound form, the sensor interacts with the ligand. The graphs show relative emission values for the inactive and the active biosensor states detected in the CFP and FRET channels when the CFP excitation wavelength is used. (**b**) The graph shows a schematic representation of the relative ratio values for various controls during biosensor optimization. The actual values would depend on the specific biosensor and the microscopy setup. From left to right: the "no FRET" situation when CFP and YPet proteins are expressed in equal amounts; the inactive biosensor with its sensor domain permanently bound to GDP (insensitive to GEFs); the wild-type biosensor existing in two different states: active and inactive; the active biosensor with its sensor domain permanently bound to GTP (insensitive to GAPs) and therefore bound to the ligand domain; the permanent FRET between CFP and YPet linked with a short linker

two additional protein domains: a ligand and a sensor that can interact when the sensor is activated (Fig. 1a). In the inactive state of a biosensor, its sensor domain is bound to the GDP and there is no interaction between the ligand and the sensor domains, which keeps two fluorophores apart resulting in low FRET values. Upon activation caused by the exchange of GDP with GTP, the GTP-loaded sensor binds to the ligand, which results in a conformational change within the biosensor bringing donor and acceptor closer to one another that causes an increase in FRET signal (Fig. 1a) [4, 11]. The most commonly used donor and acceptor pair in a FRET biosensor is cyan (CFP) and yellow (YFP) variants of the green fluorescent protein; however other fluorophore combinations are also possible [4, 18]. The position of the fluorophores

with respect to the ligand and sensor domains can vary depending on the specific biosensor design [15, 16].

What would be the best combination for CFP and YFP variants in a biosensor? One of the most important properties of intramolecular FRET biosensors is their dynamic range, which is defined as the difference between the active and inactive states of the biosensor, which in turn relies on the effectiveness of energy transfer between the donor and acceptor. Dynamic range is directly related to the sensitivity of the biosensor. Several molecular modifications have improved significantly the yellow and cyan fluorophores in terms of their brightness, stability, and the capacity to participate in energy transfer [19, 20]. We have tried different combinations of CFP and YFP variants in our FRET experiments using Rac biosensor backbone to find the pair exhibiting the best dynamic range. While the combination YPet-CyPet displayed the strongest FRET efficiency [12, 20], we do not advise using this pair in the intramolecular FRET biosensor because of a strong reduction in signal intensity in the CFP channel during the energy transfer, which makes it difficult to obtain sufficient signal level for the ratio imaging. When signal intensity is below certain level, artifacts may be caused during ratio image generation. In our hands, the best results are obtained with SECFP-YPet combination [12, 17] while other research groups use CyPet-YPet combination [20, 21].

There are several important aspects to consider when using FRET biosensor in living cells and tissues. A FRET biosensor must meet the following criteria: (1) neutrality: a good FRET biosensor should not interfere with the normal cell physiology and endogenous signaling pathways; (2) availability: the biosensor must be accessible to the activation/deactivation machinery of the cell the same way as the endogenous protein is; (3) localization: the biosensor must localize within the cell similarly to the endogenous protein; (4) dynamic range: it is important to detect significant difference between inactive and active states of the biosensor while the activity measured with the wild-type biosensor should fall between the values obtained when using the inactive and active states (Fig. 1b, *see* **Notes 1–5**).

There are multiple strategies to measure FRET efficiency that include acceptor photobleaching, sensitized emission, fluorescence lifetime measurement, and other techniques [1, 22, 23]. Here, we focus on the sensitized emission as one of the most common methods used to measure FRET when imaging live samples in a fluorescence microscope. When measuring sensitized FRET emission, the sample expressing FRET biosensor is excited at the CFP excitation wavelength and two emission channels are acquired: the CFP emission and the FRET emission. In the FRET channel, the emission measured is composed of three components: the CFP

emission that bleeds through the YFP channel, the YFP emission due to a non-direct excitation, and the YFP emission caused by the energy transfer. In case of intermolecular FRET, additional controls are required to estimate the nonspecific signal from both the donor and the acceptor in the FRET channel [24]. For intramolecular FRET biosensor, the stoichiometric ratio between the CFP and YFP fluorophores is 1; therefore the only controls needed are those for the active and the inactive states of the biosensor to define the range between the low and the high activation levels [12, 16] (Fig. 1b, *see* **Note 6**).

The main challenge when using FRET biosensors in live cells and particularly in live animals is to achieve sufficient level of signal-to-noise (S/N) ratio in the images. The expression level of a biosensor in live embryos might be low due to the toxicity or insufficient time for fluorophore synthesis and folding, which is the case when studying early developmental stages. To overcome this, several options are available. When using a camera to acquire images, use higher binning to increase the signal level; when using a confocal microscope, use higher pixel size and slower speed of scanning. In case of the early stages of zebrafish embryonic development, we suggest delaying the desired stage by incubating the embryos at lower temperature (25 °C instead of 28 °C)—that would delay the required stage allowing more time for fluorophore production/folding (*see* **Note 7**).

Here we describe the protocol for FRET ratio imaging in live zebrafish embryos using FRET biosensor for visualizing Rac activity. First, we provide a brief overview of the experimental setup and working conditions when using FRET biosensors in live embryos; then we present the ratio generation algorithm and discuss the possible pitfalls during this process; finally, we provide a macro, which can be used for analyzing large sets of data in an automated fashion. This protocol can also be used for ratio imaging in other applications since the principles of dividing one image by another are the same. While here we focus on working with RacFRET biosensor in zebrafish embryos, the same principles will apply when using other FRET biosensors in different animal models or in cell culture conditions.

2 Materials

Depending on the developmental stage, the experiment may take between several hours and several days. For early developmental stages (until 6 h post fertilization), it would be ideal to use a transgenic line, in which the FRET biosensor is maternally expressed. That would allow enough time to accumulate the

sufficient protein level in the embryo for ratio imaging. Injecting a purified protein into one-cell-stage fertilized embryo is another option for working with the early stages.

2.1 Zebrafish Work

1. Zebrafish embryos: transgenic embryos expressing the biosensor or wild-type embryos for injection with sense mRNA are collected in the morning and used for further manipulations.
2. Embryo medium: zebrafish embryos are maintained in the embryo medium [25, 26].
3. Custom-made ramps to make agarose molds for imaging: for upright microscope setups, we use custom agarose molds adapted to the embryo size.
4. Ultrapure-grade agarose to make mounting molds.
5. Low-melting agarose: used in certain mounting setups when the embryo needs extra fixation.
6. Injection needles are made by pulling glass capillaries 1.0 mm OD.
7. Dissecting microscope equipped with the fluorescence source, i.e., Leica MZ10F.

2.2 Molecular Biology

1. DNA encoding RacFRET biosensors: wild-type, positive, and negative controls relevant for the specific biosensor and fluorophores. For RacFRET, we use RacV12FRET as a positive control for high level of activation and RacN17 as a negative control for low level of activation. RacN17 mutant is expressed together with the wild-type biosensor [12].
2. mMessage machine for synthesizing capped mRNA with sp6 or T3 polymerases depending on the minimal promoter used.
3. Phenol red (optional).

2.3 FRET Ratio Imaging Setup Using Wide-Field Illumination

1. Fluorescence microscope able to acquire two images simultaneously: The DualView Imager [27] (*see* **Note 8**) and a cooled CCD camera were used to acquire the sample images provided in this chapter.
2. Optical configurations for the filter wheel and the DualView (*see* **Note 8**):
   (a) YFP filter cube for identifying cells expressing FRET biosensor: exciter 500AF25, dichroic 525DRLP, and emitter 545F35.
   (b) FRET filter cube used in the microscope filter wheel in a combination with the DualView for obtaining CFP and FRET emission values: exciter 440AF21 and dichroic 455DRLP; the emission filter is removed.

(c) DualView is fitted with 505dcxr beam splitter, ET 480/40 nm and ET 535/40 emission filters for CFP and YFP channels respectively.

3. Fluorescence excitation source for wide-field microscopy (*see* **Note 9**).
4. Objective lens: Plan-Apochromat water-dipping lens, e.g., 20x or 40x (1.0 NA).

2.4 FRET Ratio Imaging Setup Using Confocal Fluorescence Microscopy

The confocal microscope should be equipped with:

1. A laser line required to excite the donor: 458 nm for CFP excitation.
2. At least two detectors (PMT or GaAsP) to detect CFP and YFP emissions simultaneously.
3. An objective: the same as in Subheading 2.3, **step 5**.

2.5 Software and Macro for Ratio Image Generation

The present algorithm is based on *Fiji* version 1.52 g [28, 29] and requires the following plug-ins:

1. NucMed [30].
2. TurboReg [31, 32].
3. MultiStackReg (normally provided with the original *Fiji* package) [33].
4. Ratio Plus [34].
5. The macro containing the ratio algorithm can be downloaded from GitHub [35]. This algorithm is adapted for either single plane or time series images acquired in a wide-field microscope equipped with the DualView.

2.6 Sample Images

Four sets of raw data are provided for practising the ratio image generation protocol and can be downloaded from the Springer website.

1. Single-frame images showing wild-type polarized germ cells in zebrafish (shown in Figs. 2, 3, and 4):
   "Wild_Type_CFP.tif" and "Wild_Type_FRET.tif".
2. Time-lapse movie containing a wild-type zebrafish migrating germ cell, separated in two channels: "Wild_Type_Movie_CFP.tif" and "Wild_Type_Movie_FRET.tif".
3. Single frames of zebrafish somatic cells expressing the activated form of the RacFRET biosensor, to be used as positive control (*see* Fig.4): "Active_CFP.tif" and "Active_FRET.tif".
4. Single frames of zebrafish somatic cells expressing the negative form of the RacFRET biosensor, to be used as negative control (*see* Fig. 4): "Inactive_CFP.tif" and "Inactive_FRET.tif".

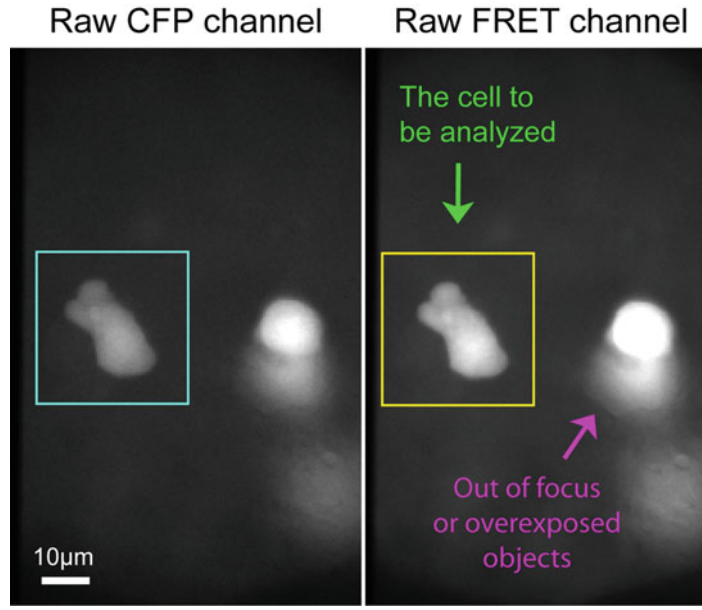

Fig. 2 Image processing **steps 1–4**. The original raw data corresponding to CFP and FRET channels are shown. These images were acquired simultaneously on the Zeiss Axioplan microscope equipped with the DualView camera set at binning 4. Images used: Files "Active_CFP.tif" and "Active_FRET.tif". ROI selection suggestion, dimensions: 65 × 65 (px). Scale bar: 10 μm

3 Methods

3.1 FRET Biosensor Expression in Zebrafish Embryos

1. Zebrafish work should be carried out according to the instructions in [25, 26].
2. Inject embryos with mRNA for RacFRET biosensor into a single cell at 8- or 16-cell stage to create mosaic labeling or use transgenic embryos expressing a biosensor. A detailed protocol for zebrafish embryo injection is described elsewhere [36].
3. Raise embryos to the desired stage (typically between 8 and 40 h post fertilization).
4. Select positively labeled embryos using a dissecting microscope equipped with the fluorescent excitation source. We prefer to use YFP filter because YFP signal is the brightest. Important: Use the lowest illumination intensity possible because FRET is highly sensitive to the bleaching (*see* **Note 9**).
5. Remove the chorion using forceps.
6. Mount the embryos in the orientation desired for imaging.

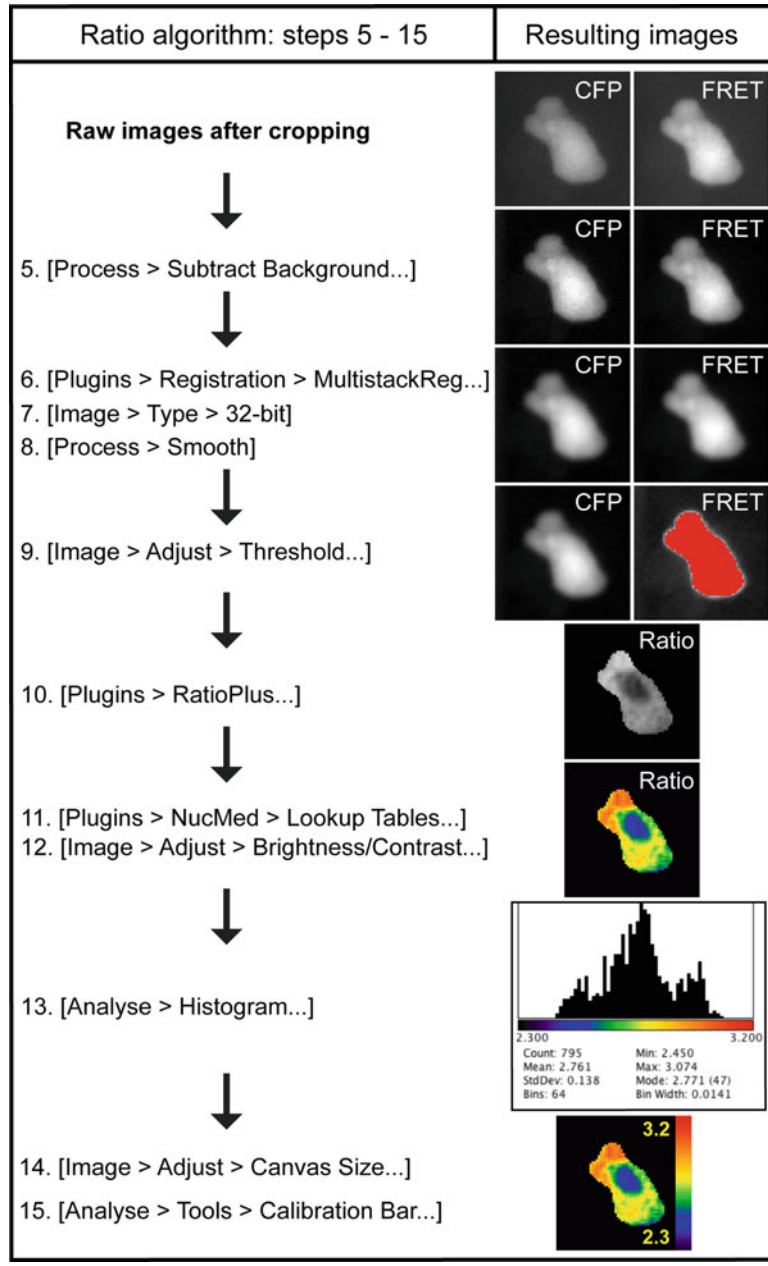

Fig. 3 Image processing **steps 5–15**. The chart shows steps in the ratio image generation algorithm after the ROI selection and cropping of the images. Resulting images for each step are shown

3.2 Image Acquisition on a Wide-Field Illumination Microscope

1. Place the mounted embryos under the microscope.
2. Use the lowest intensity illumination possible to locate the labeled cells expressing the biosensor suitable for imaging (using low-intensity illumination extremely important because

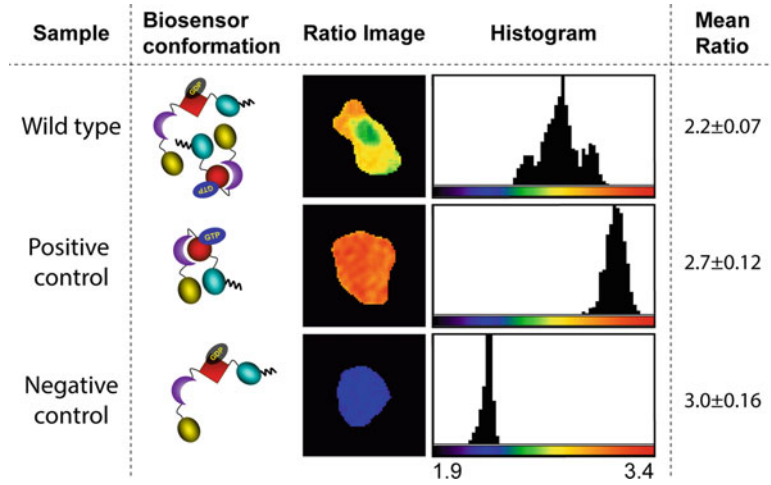

Fig. 4 Controls for RacFRET biosensor. The controls used to define the range between the active and the inactive states of RacFRET biosensor are shown. Wild type shows a migrating primordial germ cell expressing RacFRET biosensor; the positive control shows a somatic cell in a zebrafish embryo expressing RacV12FRET biosensor. V12 mutation in the Rac domain results in the biosensor that is insensitive to the GAP (GTPase-activating proteins); the negative control shows a somatic cell in the zebrafish embryo expressing a wild-type biosensor together with RacN17 mutant. The RacN17 mutant inhibits the GEF (guanine nucleotide exchange factors) preventing biosensor activation. For each control, a scheme shows the expected folding of the biosensor accompanied with the ratio image and a histogram

over-illumination would destroy FRET) as in Subheading 3.1, **step 3** (*see* **Note 9**).

3. Acquire data under the following conditions: Use FRET filter cube for CFP excitation and simultaneous acquisition of CFP and YFP emission channels in the DualView to generate CFP and FRET images, respectively. Make sure that there is no saturation in the recorded channels (*see* **Note 10**). When optimizing imaging conditions for the first time, acquire samples with the positive and negative controls to establish the dynamic range of the biosensor.
4. Acquire sufficient number of events at each developmental stage for making statistical analysis (*see* **Notes 11** and **12**).

3.3 Image Acquisition on a Confocal/Two-Photon Microscope

1. Place the sample under the microscope. In case of using fluorescence source for locating the labeled cells, use the lowest possible illumination to locate the object to be imaged.
2. When optimizing imaging conditions, we recommend using low-resolution scanning format (256 × 256 pixels) and trying pinhole apertures higher than 1 AU as well as different

acquisition speeds, in order to find the best combination that achieves the best S/N ratio.

3. Acquire data following the same principles as in **step 4**, Subheading 3.2.

3.4 Image Processing and Ratio Image Generation Algorithm

During image processing, the FRET/CFP ratio image is produced from the raw data images in a series of processing steps using *Fiji* software. The steps listed below can be executed manually or automatically using a macro provided in Subheading 2.5. Each step during image processing and ratio generation algorithm is aimed at improving the image quality as well as correcting for possible artifacts. Wrongly executed, these can cause more artifacts. We advise first-time users to run the algorithm manually step by step before applying the accompanying macro for automated ratio image generation. This exercise will help to understand the function of each step as well as to detect possible errors that may arise during this process.

1. Launch *Fiji*.
2. Open the image files corresponding to the FRET and CFP channels or the respective stack images in case of a time lapse at [File > Open...] or drag the image files directly into *Fiji*.
3. Select the appropriate region of interest (ROI) containing the cell or group of cells to be analyzed. Avoid overlapping, saturated, or out-of-focus cells next to the one to be analyzed (Fig. 2). Use the FRET image to generate the ROI using [Edit > Selection > Specify...]. Select the *Width* and the *Height* to include the object to be analyzed and to ensure sufficient area around the cell for background correction. For the images provided here, anything between 65 × 65 and 75 × 75 (in pixels) would be suitable. To store the ROI, select [Analyze > Tools > ROI Manager...], press *Add*, and the respective ROI will appear in the *ROI Manager* window. A quicker way to activate the *ROI Manager* window is by pressing *t* on the keyboard. Switch to the CFP image and select the ROI within the *ROI Manager* box to activate the ROI at the same location as in the other image. Another way to place the ROI at the same location in the other image is to press *shift e* on the keyboard after switching to the second image.
4. Crop the images: [Image > Crop] (*see* **Note 13**).
5. Correct the background for uneven illumination. It should be applied to both images. In case of acquiring images in the widefield microscope, uneven illumination is very common. To correct it, we suggest using the rolling ball algorithm implemented in *Fiji* at [Process > Subtract Background...]. The typical range for the *Rolling ball radius* is between 50 and 200 px (*see* **Note 14**). Press *OK*.

6. Register the two channels. This step is necessary when two channels are misaligned, which is often the case when using the DualView on a wide-field microscope (*see* **Note 15**). *MultiStackReg* works for both single images and stacks. This can be done at [Plugins > Registration > MultiStackReg...]. Select the CFP image or stack as *Stack 1* and set *Use as Reference* in *Action 1*. Select the FRET image or stack as *Stack 2* and set *Align to First Stack* in *Action 2*. Select *Rigid Body* for transformation.
7. Convert images to 32 bits at [Image > Type > 32-bit] (*see* **Note 16**). This step should be applied to both images.
8. Filter the images using [Process > Smooth]. Filtering is often used during image processing to reduce the background noise. We use a smooth filter, which is a mean filter of radius 1 (*see* **Note 17**).
9. Segment the images. This step is necessary to avoid artifacts in the background during ratio image generation at a later step. During segmentation, the minimum and the maximum intensity values are set and the values outside the threshold are ignored. This is done at [Image > Adjust > Threshold...]. Select the *Default* algorithm and tick the options *Red* and *Dark Background*. In case of working with stacks, select *Stack Histogram*, which is necessary to avoid artifacts caused by the intensity variations due to bleaching. Then press *Apply* and tick *Set background pixels to NaN* when prompted to convert all background pixels to NaN (not a number). NaN pixels will be discarded in any image calculation (*see* **Note 16**).
10. Generate the ratio image using [Plugins > RatioPlus...]. Choose the FRET image as *Image 1* and the CFP image as *Image 2*. Press *OK*. We recommend saving this image as *.tif* file and perform further manipulations (next steps) such as adjusting the intensity range and preparing the image for presentation on a duplicate of this ratio image.
11. Assign a lookup table (LUT) to the ratio image using the *NucMed* plug-in, which offers a large variety of LUTs in addition to those already integrated in *Fiji*. This plug-in can be found at [Plugins > NucMed > Lookup Tables]; choose *Blue Green Red* from the list under *LUT name*.
12. Adjust the intensity range of the ratio image using [Image > Adjust > Brightness/Contrast...]. Press *Set* in the "B&C" window and type in the desired values. Here we used 2.3 and 3.2 as low and high values, respectively (*see* **Note 18**). Duplicate the ratio image, convert it to RGB, and save it for presentation purposes.
13. Show the histogram of the ratio image. The histogram is a useful tool to obtain the mean and the max/min values, and

to visualize the noise in the images by the spread of the intensity values. It also serves for visual representation of the biosensor range (Figs. 3 and 4). This function is found at [Analyze > Histogram]. In the *Histogram* window, use 100 bins, unselect the *Use pixel value range*, and set up the same *X min* and *X max* values as chosen for the range in the previous step.

14. Increase the canvas or image size. This step will increase the background space in the image to prepare it for use in presentations and figures. This extra space is necessary for instance to add a calibration bar (added in the next step) to fit into the image or any additional information such as the specific condition. There are two options to do it, either resizing the canvas of the image using [Image > Adjust > Canvas Size...] or resizing the entire image at [Image > Adjust > Size...] using *Constrain aspect ratio*, *Average when downsizing*, and *Interpolation: None*. In both cases, it is required to type in the new parameters for *Width* and *Height*. In this protocol, the image was resized to 400 px width.
15. Add a calibration bar to the ratio image. This step would place a colored calibration bar showing the ratio intensity differences on the image. This function can be found at [Analyze > Tools > Calibration Bar...]. The options used in this protocol are: *Location: Upper Right*; *Fill color: Black*; *Label color: White*; *Number of Labels: 3*; *Decimal places: 1*; *Font size: 14*; and *Zoom factor: 1.5*.

3.5 Macro for the Automated Processing

All the steps described in Subheading 3.4 can be easily automated by using the macro recorder in *Fiji* at [Plugins > Macros > Record...]. The recorder keeps track of all the functions called and allows for creating a script that automatically repeats the whole procedure over the same set of images. Such basic script needs to be further edited to make it usable with other sets of images and, to that aim, some new functionalities may be required. This section describes step by step all such functionalities that have been added to the recorded script in order to create the provided macro. Although no programming detail is particularly granted, the specific blocks of the code are shown in Figs. 5, 6, 7, and 8 to complement the information given at each step, and to be used as example in other programming pipelines.

1. Open the macro or drag and drop it to the *Fiji* bar and press *Run* in the script editor window.
2. Before opening an image, the macro pops up a dialog box (Fig. 5a) where the minimum and maximum ratio values should be introduced (*see* **Note 18**). These values will be stored in two variables and will be used in the latest macro steps to adjust the brightness and contrast of the ratio image. The

A

```
//Create the dialog box asking for ratio values
Dialog.create("FRETRatioAnalysis");
Dialog.addNumber("Minimum value for the ratio", 1.9);
Dialog.addNumber("Maximum value for the ratio", 3.4);
Dialog.show;
minRatio = Dialog.getNumber();
maxRatio = Dialog.getNumber();
```

B

```
//Open FRET image, collect data and open its corresponding CFP image
showMessage("Open a FRET image when asked");
open();
title = getTitle();
fretID = getImageID();
input = File.directory;
experiment = substring(title, 0, lengthOf(title)-8);//Removing FRET and file extension
cellType = substring(title, lengthOf(title)-8, lengthOf(title)-4);//Looking for FRET word
extension = substring(title, lengthOf(title)-4);//Looking for file extension
getDimensions(width, height, channels, slices, frames);
if(cellType=="FRET"){
  open(experiment + "CFP" + extension);//Pair of FRET image previously open
  cfpID = getImageID();
}else{
  exit("There is no FRET image open");
}
```

C

```
//Calculate the ratio
run("Ratio Plus", "image1=[FRET] image2=[CFP] background1=0 clipping_value1=0 background2=0 clipping_value2=0 multiplication=1");
ratioID = getImageID();
setMinAndMax(minRatio, maxRatio);
```

Fig. 5 Macro blocks, part 1. (**a**) This set of commands creates a dialog box to ask for the minimum and maximum values of the ratio range. These values are stored in two variables, "minRatio" and "maxRatio", respectively. (**b**) This code block asks to select a FRET image to be opened and then stores its dimensions, name, path, and ID in variables. Afterwards, the macro checks whether this image corresponds to the FRET channel and opens the matching image corresponding to the CFP channel; otherwise, an error message appears and the macro stops. (**c**) This set of commands creates a ratio image with the range of values predetermined in (**a**)

default values shown are fine for the current sample images. Once the values are entered, press the *OK* button to proceed.

3. The next macro block (Fig. 5b) is aimed to open the FRET image. A message is shown warning about this. After pressing *OK* the macro forces the computer browser to pop up for the FRET image to be selected. Once opened, the file's general information (dimensions, name, image ID, and path to the input folder) is collected. The macro then checks whether the

A

```
88 //Add a calibration bar
89 selectImage(ratioID);
90 run("Lookup Tables", "resource=Lookup_Tables/ lut=[Blue
   Green Red]");
91 run("Duplicate...", "title=copy duplicate");
92 resizeImage();
93 run("Calibration Bar...", "location=[Upper Right]
   fill=Black label=White number=3 decimal=1 font=14
   zoom=1.5 overlay");
94 run("Flatten", "stack");
95 calBarID = getImageID();
```

B

```
128 //Function to resize an image and increase its canvas
    by 100px width
129 function resizeImage(){
130   if(width<400){
131     run("Size...", "width=400 height=400 constrain
        average interpolation=None");
132     height = getHeight();
133   }
134   width = getWidth() + 100;
135   run("Canvas Size...", "width="+width+"
      height="+height+" position=Center-Left zero");
136 }
```

Fig. 6 Macro blocks, part 2. (**a**) This portion of macro applies a LUT to the ratio image, duplicates and resizes it, and adds a calibration bar. (**b**) This user-defined function named *resizeImage()* is used to resize and modify the canvas size of the active image

image contains the word "FRET" in its name and then for its partner (CFP image) in the same input folder. In case the selected image is not a "FRET" one, the macro shows an error message and stops (*see* **Note 19**).

4. Both of the open images are renamed as "FRET" and "CFP" to facilitate further operations with them inside certain *Fiji* functions (i.e., **step 5**).
5. The macro pops up a message window asking the user to draw a ROI around the cell of interest in the "FRET" image. Once drawn, press *OK* in the message window and the macro will draw the same ROI in the "CFP" image.
6. **Steps 4–9** in Subheading 3.4 are then executed and the macro controls the action at every step and the specific image it is applied to.
7. The macro calls the *Ratio Plus* function using the "FRET" and "CFP" names generated earlier in **step 3** (Fig. 5c, line 84).
8. The brightness and contrast of the ratio image (obtained in **step 5**) are adjusted using the minimum and maximum values defined at the beginning of the macro execution (Fig. 5c, line 86).

A

```
97  //Obtain histogram
98  selectImage(ratioID);
99  rename("Ratio");
100 if(slices>1){
101   stackHistogram();
102 }else{
103   run("Histogram", "bins=100 x_min=" + minRatio + "
      x_max=" + maxRatio + " y_max=Auto");
104 }
```

B

```
138 //Function to create a stack of histograms obtained
    from each slice in a stack
139 function stackHistogram(){
140   setBatchMode(true);
141   for(i=1; i<=slices; i++){
142      selectImage(ratioID);
143      setSlice(i);
144      run("Histogram", "bins=100 x_min=" + minRatio + "
         x_max=" + maxRatio + " y_max=Auto");
145      rename("frame " + i);
146   }
147   run("Images to Stack", "name=histoStack title=frame
      use");
148   rename("Histogram of Ratio");
149   setBatchMode(false);
150 }
```

Fig. 7 Macro blocks, part 3. (**a**) This set of commands creates the histogram with the range of values defined in Fig. 5a, lines 25 and 26. (**b**) This user-defined function named *stackHistogram()* is used to obtain a histogram from each slice of a stack and then combine all histogram images into a new stack

A

```
106 //Create Results folder inside the input folder
107 output = input + "Results" + File.separator;
108 File.makeDirectory(output);
109 if(!File.exists(output)){
110   exit("Unable to create the folder");
111 }
```

B

```
113 //Save images and histogram
114 selectImage(calBarID);
115 saveAs("Tiff", output + experiment + " Ratio_RGB");
116 selectImage(ratioID);
117 saveAs("Tiff", output + experiment + " Ratio");
118 selectWindow("Histogram of Ratio");
119 saveAs("Tiff", output + experiment + "
    Ratio_Histogram");
120 if(isOpen("copy")){
121   selectWindow("copy");
122 close();
```

Fig. 8 Macro blocks, part 4. (**a**) This code creates an output folder named "Results" inside the input folder selected in Fig. 5b. (**b**) This set of commands saves the original ratio image, its copy with the calibration bar, and the histogram inside the "Results" folder created in (**a**)

9. After applying the LUT, the ratio image is duplicated and then resized using a user-defined function named *resizeImage* (Fig. 6a, line 92). This function is defined at the end of the macro (Fig. 6b, lines 129–136) and it is used to resize an image in case it is smaller than 400 px width and finally enlarge the width of the canvas by 100 px (*see* **Note 20**).
10. The calibration bar (Fig. 6a, line 93) is accommodated in the upper right corner of this resized image. First it is added as an overlay to the ratio image and then both calibration bar and image are flattened to obtain an RGB image.
11. The histogram for the ratio image is generated using the minimum and maximum values entered at the beginning of the execution of the macro (Fig. 7a). If the ratio image is a stack the macro calls another user-defined function named *stackHistogram()* (Fig. 7a, line 101). This function is defined at the end of the macro (Fig. 7b, lines 139–150) and it is used to generate a histogram of each slice and finally to convert all histograms into a stack.
12. The macro creates an output folder named "Results" inside the input folder where the original images are located (Fig. 8a).
13. Finally, the ratio image, its duplicate with the calibration bar created in **step 8**, and the histogram are saved inside the output folder created in **step 10** (Fig. 8b).

4 Notes

1. FRET biosensors are unique tools that allow obtaining instant information about protein activity and signaling events in living organisms. Experiments involving FRET biosensors are complex and require multiple steps, each step involving another discipline: molecular biology and animal work to optimize the biosensor expression in a living tissue; microscopy for observation and image acquisition; and computer-assisted image processing for analyzing the raw data. Each of these steps brings specific challenges and here we describe the most common ones and offer possible solutions. We do not discuss the principles of the molecular design for FRET biosensors because these are far beyond the scope of this protocol.
2. Toxicity: The biosensor should not cause any adverse effects such as cell death, abnormal shape, interference with proper cell cycle, and other normal cellular functions. Therefore, the very first experiment when working with biosensors involves expressing it in the embryo either globally or in the population of cells and monitoring proper development. Ideally, there should be no difference between embryos expressing the

biosensor and the embryos expressing a control protein that is known to be nontoxic.

3. Neutrality: The biosensor should not interfere with the endogenous signaling processes within the cells. While one can never be 100% sure that no other signaling pathways are affected by the biosensor overexpression, a simple observation of cellular shapes, rate of cell division, and proper animal development should indicate if the biosensor might be causing developmental abnormalities due to signaling interference. For example, in case of migrating cells, the proper migration should be a good indication that the biosensor is not interfering with important signaling events. Other examples might include a proper shaping of the targeted tissues and the expression of relevant markers in the presence of a biosensor.
4. Subcellular targeting: The biosensor should be localized in the same subcellular areas as the corresponding endogenous protein. This can be tested by comparing the subcellular distribution of the overexpressed biosensor with the expression pattern of the endogenous protein probed by an antibody staining. If the antibody is not available, a GFP fusion of the corresponding protein can be used as an alternative. In case of Rho GTPases, the C-terminal farnesylation site of the respective Rho GTPase fused to the 5′ of the biosensor was used to ensure the proper localization to the membrane where these proteins normally carry out their work [11]. Depending on the tissue and cell types, the biosensor localization might require further optimization. For example, in zebrafish germ cells, the original FRET biosensor for Rac protein had shown the predominant accumulation in the nucleus and several modifications such as eliminating the nuclear localization sequence in the Rac farnesylation site or a deleting this C-terminal domain were made to ensure a proper targeting [17]. Additional considerations for optimizing biosensor for subcellular targeting and proper functioning include changes in the order of different modules in a biosensor backbone [16, 21].
5. Availability and responsiveness: The biosensor should be accessible and responsive to the endogenous activation and deactivation machinery that acts on the corresponding protein. This can be tested by measuring FRET in the presence of one of the known activators of the protein studied. In case of RacFRET biosensor, we have used the active domain of Tiam1, one of the Rac activators [17].
6. Controls: For each biosensor, the controls for the active and inactive state will help defining the range between high and low FRET levels. Even in the inactive state of the biosensor, a low FRET level will be detected in many cases; therefore a sample

expressing CFP and YFP fluorophores cannot serve as a negative control (Fig. 1b). For the very first optimization of FRET measurements when using new equipment/conditions, it is recommended to use additional controls that will allow distinguishing between no FRET and a constant FRET (Fig. 1b).

7. Signal to noise level: When dividing one image by another, high signal intensity in the images is crucial. When signal intensity drops below certain level, which is at least double of the background noise, artifacts may arise during the division. Typically, the CFP channel is expected to have the lowest intensity level because CFP variants in general have lower quantum yield as compared with YFP variants and in addition the CFP signal will be reduced due to the energy transfer. It can also be difficult to achieve high signal intensity in the embryos because of the possible toxic effects of the high number of biosensor molecules to the embryo. To overcome these, we recommend several strategies:
   (a) Use brighter CFP and YFP variants. Many CFP and YFP variants were created showing an improved brightness and energy transfer [20]. These were successfully utilized in biosensors.
   (b) Delay embryonic development by lowering the temperature. In case when the observation takes place at the early developmental stages (before 8 h post fertilization), the shorter incubation time may compromise the biosensor brightness due to the time it takes for the fluorophore folding and maturation. Keeping the embryos at a lower temperature (24 °C instead of 28 °C for zebrafish embryos) would delay the embryonic development and add the time required for biosensor signal accumulation.
   (c) When possible, use transgenic animals instead of mRNA injection for a transient expression. In transgenic animals, the signal-to-noise ratio is often higher as compared to mRNA injection. Also, transgenic technology allows targeting specific tissues and cell populations, which can be helpful in improving the signal.
8. DualView is an optical device that allows simultaneous acquisition of two spectrally distinct images, therefore avoiding any lag between the acquisition of the two images and minimizing the photo-destruction of fluorophores during the acquisition process. The filter configurations proposed here are optimal for the CFP/YFP FRET pair. If different fluorescent proteins are used as FRET pair in a biosensor, these configurations must be adjusted using the respective excitation/emission parameters for specific fluorophores [18].

9. Bleaching is the worst enemy of FRET because strong illumination destroys energy transfer between two fluorophores; therefore samples expressing FRET biosensors should never be exposed to a strong fluorescence source. Avoid bleaching by reducing the intensity of the fluorescence excitation source. We recommend using about 25% or less of the available fluorescence intensity. This can be achieved by reducing the power of the fluorescence or by fitting optical density filters in front of the fluorescence source.
10. Saturation: Another enemy of FRET is signal saturation. Saturated images cannot be used for quantitative data analysis because they do not contain the correct intensity values. Saturation normally occurs in the FRET channel and can be detected by the apparent uniform signal in the image or using pseudo color lookup tables in the image acquisition software that present saturated pixels during data acquisition.
11. Number of cells to be analyzed: We recommend measuring at least 30 cells for each condition, especially when optimizing imaging conditions and establishing the range for biosensor activity (*see* Subheading 3.4 and **Note 18** for further details on image processing). This would allow to account for data variability when establishing the dynamic range of the biosensor and comparing between different cell types, developmental stages, or other conditions such as mutants or drug treatments.
12. When working with live embryos, we observed an increase in average FRET level in biosensors during time. This increase is not biosensor related because we observe it as well in the SECFP-YPet fusion module, which cannot depend on the external activators [12]. Therefore, it is important to perform every set of measurements at the same developmental stage when working with embryos.
13. After the images were cropped, it is not possible to go back to the original image except for opening it again. In a multistep protocol such as ratio image generation, it can be useful to duplicate the region of interest instead of cropping the images and work on a copy. That would allow going back to the original images and start over in case there was an error at one of the steps.
14. Background correction: Uneven illumination in a wide-field microscope will result in variations in intensity across the image. This noise can be corrected with the *Subtract Background* function implemented in *Fiji*. This function employs a rolling ball algorithm [37]. The *Rolling ball radius* (in pixels) should be larger than the largest object in the image that is not part of the background. In case of the confocal imaging, the background noise in the detectors can be corrected by

subtracting a fixed value from each pixel of the image corresponding to the background signal level: [Process > Math > Subtract...].

15. Registration: During registration, two images or two stacks are aligned and shifts along *x*- and *y*-axes are corrected. In a wide-field microscope, it is often the case that the CFP and FRET channels are shifted relative to one another, especially when the DualView is used. When two images are misaligned, the ratio image will contain artifacts, which might be misinterpreted as real data. A typical artifact in the ratio image caused by the division of two misaligned images would manifest as abnormally high and low values at the opposite edges of the cell.
16. 32-bit conversion: Original raw data generated in a microscope would typically be in 8-bit or 16-bit format. The conversion to 32 bits allows conversion of the background pixels to NaN (not a number) during the segmentation step and retaining the intensity information within the object. This allows saving time instead of creating a mask separately and multiplying it to the original images. More importantly, the 32-bit conversion generates floating numbers, which is essential when dividing one image by another as it allows decimal numbers.
17. Filters are used to reduce the noise and to improve the image quality. However, it may introduce artifacts or result in data loss. We prefer using the *Smooth* filter in this protocol for its mild effects on averaging the data during filtering. It is possible to use other filters such as *Gaussian Blur* and *Median* if necessary; however we do not recommend applying radius larger than 2 px to avoid artifacts.
18. Defining the dynamic range between the active and inactive states in the RacFRET biosensor: The range values are defined based on the measured ratio values in each specific experiment using positive and negative controls that should provide low FRET and high FRET values. For the visual representation, it is recommended to set the range at values slightly lower than the minimal and slightly higher than the maximum values measured for the inactive and the active biosensor states. In that case, the cell expressing the inactive biosensor form will be clearly visible on the dark background (Fig. 4). It is expected that the active and inactive controls would have a very narrow range shown in their histograms as compared with the wild-type situation. The range in the controls reflects the noise in the biosensor and should be smaller as compared to the wild-type situation (Fig. 4).
19. The ratio image in this protocol is performed dividing a pair of images. To avoid mistakes when opening the two required images, we programed the macro to ask for a FRET image

and then the macro itself opens its partner, i.e., the CFP image. To be able to do so, the name of the images must end in "FRET" and "CFP", respectively (Fig. 5b): for example "MyControl_FRET.tif" and "MyControl_CFP.tif".

20. Cropping the images to select only the cell or cells of interest performed in this protocol results in images sizing less than 400 px.

Acknowledgments

Elena Kardash is grateful to Dr. Nadine Peyriéras at CNRS/BioEmergences and her laboratory for providing support during the creation of this chapter. E.K. was supported by the ANR-10-INBS-04 through the National Infrastructure France-BioImaging supported by the French National Research Agency and by the 2017-ITN-721537 as part of the ITN ImageInLife Marie Skłodowska-Curie Actions when working on this chapter.

References

1. Lakowicz JR (2007) Principles of fluorescence spectroscopy. Springer, New York
2. Clegg RM (2009) Förster resonance energy transfer—FRET what is it, why do it, and how it's done. In: FRET and FLIM techniques, Laboratory techniques in biochemistry and molecular biology, 33, 1st edn. Elsevier, Amsterdam
3. Okamoto K, Sako Y (2017) Recent advances in FRET for the study of protein interactions and dynamics. Curr Opin Struct Biol 46:16–23
4. Ni Q, Mehta S, Zhang J (2018) Live-cell imaging of cell signaling using genetically encoded fluorescent reporters. FEBS J 285:203–219
5. Miyawaki A, Llopis J, Heim R, McCaffery JM, Adams JA, Ikura M, Tsien RY (1997) Fluorescent indicators for Ca2+ based on green fluorescent proteins and calmodulin. Nature 388:882–887
6. Kurokawa K, Ohba Y, Nagal T, Miyawaki A, Matsuda M (2001) Spatio-temporal images of growth-factor-induced activation of Ras and Rap 1. Nature 411:1065–1068
7. Miyawaki A (2003) Visualization of the spatial and temporal dynamics of intracellular signaling. Dev Cell 4:295–305
8. Kiyokawa E, Aoki K, Nakamura T, Matsuda M (2011) Spatiotemporal regulation of small GTPases as revealed by probes based on the principle of Förster Resonance Energy Transfer (FRET): implications for signaling and pharmacology. Annu Rev Pharmacol Toxicol 51:337–358
9. Shimozono S, Iimura T, Kitaguchi T, S-i H, Miyawaki A (2013) Visualization of an endogenous retinoic acid gradient across embryonic development. Nature 496:363–366
10. Haga RB, Ridley AJ (2016) Rho GTPases: regulation and roles in cancer cell biology. Small GTPases 7:207–221
11. Itoh RE, Kurokawa K, Ohba Y, Yoshizaki H, Mochizuki N, Matsuda M (2002) Activation of Rac and cdc42 video imaged by fluorescent resonance energy transfer-based single-molecule probes in the membrane of living cells. Mol Cell Biol 22:6582–6591
12. Kardash E, Bandemer J, Raz E (2011) Imaging protein activity in live embryos using fluorescence resonance energy transfer biosensors. Nat Protoc 6:1835–1846
13. Pertz O, Hahn KM (2004) Designing biosensors for Rho family proteins—deciphering the dynamics of Rho family GTPase activation in living cells. J Cell Sci 117:1313–1318
14. Nakamura T, Aoki K, Matsuda M (2005) Monitoring spatio-temporal regulation of Ras and Rho GTPases with GFP-based FRET probes. Methods 37:146–153
15. Pertz O, Hodgson L, Klemke RL, Hahn KM (2006) Spatiotemporal dynamics of RhoA activity in migrating cells. Nature 440:1069–1072

16. Fritz RD, Letzelter M, Reimann A, Martin K, Fusco L, Ritsma L, Ponsioen B, Fluri E, Schulte-Merker S, van Rheenen J, Pertz O (2013) A versatile toolkit to produce sensitive FRET biosensors to visualize signaling in time and space. Sci Signal 6:rs12
17. Kardash E, Reichman-Fried M, Maître J-L, Boldajipour B, Papusheva E, Messerschmidt E-M, Heisenberg C-P, Raz E (2010) A role for rho GTPases and cell-cell adhesion in single-cell motility in vivo. Nat Cell Biol 12:47–53
18. Bajar BT, Wang ES, Zhang S, Lin MZ, Chu J (2016) A guide to fluorescent protein FRET pairs. Sensors (Basel):16, 1488
19. Sawano A, Miyawaki A (2000) Directed evolution of green fluorescent protein by a new versatile PCR strategy for site-directed and semi-random mutagenesis. Nucleic Acids Res 28: e78
20. Nguyen AW, Daugherty PS (2005) Evolutionary optimization of fluorescent proteins for intracellular FRET. Nat Biotechnol 23:355–360
21. Komatsu N, Aoki K, Yamada M, Yukinaga H, Fujita Y, Kamioka Y, Matsuda M (2011) Development of an optimized backbone of FRET biosensors for kinases and GTPases. Mol Biol Cell 22:4647–4656
22. Jares-Erijman EA, Jovin TM (2003) FRET imaging. Nat Biotechnol 21:1387–1395
23. Jares-Erijman EA, Jovin TM (2006) Imaging molecular interactions in living cells by FRET microscopy. Curr Opin Chem Biol 10:409–416
24. Xia Z, Liu Y (2001) Reliable and global measurement of fluorescence resonance energy transfer using fluorescence microscopes. Biophys J 81:2395–2402
25. Kimmel CB, Ballard WW, Kimmel SR, Ullmann B, Schilling TF (1995) Stages of embryonic development of the zebrafish. Dev Dyn 203:253–310
26. Westerfield M (2000) The zebrafish book: a guide for the laboratory use of zebrafish (*Danio rerio*). http://zfin.org/zf_info/zfbook/cont.html
27. DualView. https://www.photometrics.com/products/multichannel/dv2.php
28. Schneider CA, Rasband WS, Eliceiri KW (2012) NIH image to ImageJ: 25 years of image analysis. Nat Methods 9:671–675
29. Fiji. https://imagej.net/Fiji/Downloads
30. Parker JA NucMed. http://www.med.harvard.edu/JPNM/ij/plugins/NucMed.html
31. Thévenaz P, Ruttimann UE, Unser M (1998) A pyramid approach to subpixel registration based on intensity. IEEE Trans Image Process 7:27–41
32. TurboReg. http://bigwww.epfl.ch/thevenaz/turboreg/
33. Busse B MultistackReg. http://bradbusse.net/downloads.html
34. Magalhães P (2003) Ratio Plus. https://imagej.nih.gov/ij/plugins/ratio-plus.html
35. Bosch M (2018) FRET ratio. https://github.com/manelbosch76/ijm-Macros
36. Rosen JN, Sweeney MF, Mably JD (2009) Microinjection of zebrafish embryos to analyze gene function. J Vis Exp 25:1115
37. Rolling ball. http://imagejdocu.tudor.lu/doku.php?id=gui:process:subtract_background